WARM SATURNS: ON THE NATURE OF RINGS AROUND EXTRASOLAR PLANETS THAT RESIDE INSIDE THE ICE LINE

Hilke E. Schlichting[1,2,4] and Philip Chang[3]

[1] Department of Earth and Space Science, University of California, Los Angeles, 595 Charles E. Young Drive East, Los Angeles, CA 90095, USA; hilke@ucla.edu
[2] California Institute of Technology, MC 130-33, Pasadena, CA 91125, USA
[3] Canadian Institute for Theoretical Astrophysics, 60 St George Street, Toronto, ON M5S 3H8, Canada; pchang@cita.utoronto.ca

ABSTRACT

We discuss the nature of rings that may exist around extrasolar planets. Taking the general properties of rings around the gas giants in the solar system, we infer the likely properties of rings around exoplanets that reside inside the ice line. Due to their proximity to their host star, rings around such exoplanets must primarily consist of rocky materials. However, we find that despite the higher densities of rock compared to ice, most of the observed extrasolar planets with reliable radius measurements have sufficiently large Roche radii to support rings. For the currently known transiting extrasolar planets, Poynting–Robertson drag is not effective in significantly altering the dynamics of individual ring particles over a time span of 10^8 yr provided that they exceed about 1 m in size. In addition, we show that significantly smaller ring particles can exist in optically thick rings, for which we find typical ring lifetimes ranging from a few times 10^6 to a few times 10^9 yr. Most interestingly, we find that many of the rings could have nontrivial Laplacian planes due to the increased effects of the orbital quadrupole caused by the exoplanets' proximity to their host star, allowing a constraint on the J_2 of extrasolar planets from ring observations. This is particularly exciting, since a planet's J_2 reveals information about its interior structure. Furthermore, measurements of an exoplanet's J_2 from warped rings and of its oblateness would together place limits on its spin period. Based on the constraints that we have derived for extrasolar rings, we anticipate that the best candidates for ring detections will come from transit observations by the *Kepler* spacecraft of extrasolar planets with semimajor axes ∼0.1 AU and larger.

Key words: planets and satellites: detection – planets and satellites: general – planets and satellites: rings

Online-only material: color figures

1. INTRODUCTION

Ring systems exist around all of the giant planets in our solar system. The rings of the Saturnian system are the most prominent and consist mainly of centimeter- to meter-sized icy bodies (French & Nicholson 2000). On the other hand, Jupiter's rings are far more tenuous and consist of micron-sized dust particles (Showalter et al. 2008). Since rings are ubiquitous around giant planets in the solar system, they may also be common around extrasolar planets.

Although more than 500 extrasolar planets have been discovered to date, no extrasolar satellites or ring systems have been detected yet. However, this may change soon due to the unprecedented photometric accuracy of the *Kepler* satellite (Borucki et al. 2010) and due to the constantly improving precision and increasing temporal baseline of ground-based radial velocity surveys. Since rings typically reside in the planet's equatorial plane, the required photometric and spectroscopic precision for ring detection depends on the planet's obliquity. The obliquity, θ_*, refers here to the angle between an extrasolar planet's spin axis and the normal of its orbital plane. Barnes & Fortney (2004) estimate that Saturn-like rings could be detected around transiting extrasolar planets with a photometric precision of $(1–3) \times 10^{-4}$ and a 15 minute time resolution as long as the ring is not viewed close to edge-on (i.e., as long as θ_* is not ≪1). This is within the photometric accuracy that the *Kepler* spacecraft achieves for Sun-like and brighter stars (http://keplergo.arc.nasa.gov/CalibrationSN.shtml). In

addition, rings around transiting extrasolar planets could also be identified spectroscopically (Ohta et al. 2009). Ohta et al. (2009) showed that rings with significant obliquities are detectable with currently achievable radial velocity precision of 1 m s^{-1}, whereas rings with $\theta_* \ll 1$ would typically require a radial velocity precision of 0.1 m s^{-1} or less, which is still beyond the reach of radial velocity surveys.

A potential obstacle to detecting extrasolar rings may be that most close-in exoplanets could have low obliquities, which would make their rings hard, if not impossible, to discover. The initial obliquities of close-in extrasolar planets with masses comparable to and bigger than Neptune are likely to be large, since such planets are thought to have formed at larger semimajor axes and have reached their current location by planet–planet scattering, disk migration, or by Kozai oscillations with a stellar companion or a combination of such processes (e.g., Lin & Papaloizou 1979; Lin et al. 1996; Rasio & Ford 1996; Chatterjee et al. 2008; Wu & Murray 2003; Wu et al. 2007). Tides raised on the exoplanet by its host star will, however, lead to damping of its obliquity. To first order in θ_*, the obliquity damping timescale for exoplanets with small eccentricities is given by

$$t_{\text{damp}} = \theta_* \frac{dt}{d\theta_*} \sim \frac{2\alpha_P Q_P}{3k_P} \left(\frac{M_P}{M_*} \right) \left(\frac{a}{R_P} \right)^3 \Omega^{-1}, \quad (1)$$

where k_P is the exoplanet's tidal Love number, Q_P is its tidal dissipation function, M_* is the stellar mass, and a, R_P, and M_P are the semimajor axis, radius, and mass of the extrasolar planet, respectively (e.g., Hut 1981; Levrard et al. 2007). $\alpha_P = I_P/M_P R_P^2 \leqslant 2/5$, where I_P is the exoplanet's moment of

---

[4] Hubble Fellow.

inertia and Ω is its orbital frequency.[5] Since the synchronization timescale is comparable to the obliquity damping timescale, we assumed in Equation (1) that the exoplanet's spin period is comparable to its orbital period. Evaluating Equation (1) for a Jupiter-like exoplanet around a Sun-like star and assuming $Q_P \sim 10^{6.5}$ (Jackson et al. 2008) and $k_P \sim 3/2$, we find that $t_{\text{damp}} \gtrsim 10^8$ yr and $t_{\text{damp}} \gtrsim 10^9$ yr for semimajor axes greater than about 0.1 AU and 0.2 AU, respectively. We therefore expect most exoplanets with semimajor axes greater than a few tenths of an AU to have significant obliquities, allowing for ring detections. Although only a handful of transiting exoplanets are currently known with $a \gtrsim 0.1$ AU, the *Kepler* satellite is likely to fill in this parameter space in the near future. Furthermore, even for systems with $a \lesssim 0.1$ AU, stellar tides do not need to damp exoplanets' obliquities to zero, because for sufficiently high initial obliquities, the planets may settle into a high-obliquity Cassini state (Winn & Holman 2005; Fabrycky et al. 2007; Levrard et al. 2007). In short, we expect most exoplanets with semimajor axes greater than a few tenths of an AU to have significant obliquities, allowing for ring detections, and note that systems with smaller semimajor axes could reside in high-obliquity Cassini states rather than having their obliquities damped to zero.

In this paper, we investigate what types of ring systems could exist around extrasolar planets with semimajor axes of about 1 AU or less. We focus on these systems, which we coin "warm Saturns," since they fall within the *Kepler* discovery space, which is limited to extrasolar planets with orbital periods of about 1 yr and less. We show that such extrasolar ring systems, if they exist, will differ from those in our solar system and examine the different dynamical forces that play a role in shaping them. We show that the presence of extrasolar rings, or the lack thereof, provides interesting implications for ring formation theories and that the detection of extrasolar rings will constrain the extrasolar planet's obliquity and in some cases also its quadrupole moment. Measuring an exoplanet's quadrupole moment would be especially exciting since it would allow us to probe its interior structure (Ragozzine & Wolf 2009).

This paper is structured as follows. We start by determining the Roche radius and ring composition in Section 2.1 and examine the effect of Poynting–Robertson drag on the ring particles in Section 2.2. In Sections 2.3 and 2.4, we discuss the implications of the planet's proximity to its host star on ring formation and ring orientation, respectively. Discussion and conclusions follow in Section 3.

2. PROPERTIES OF PLANETARY RINGS

In this section, we discuss the general properties of planetary rings from ring studies in the solar system. We then extend these results to extrasolar planets and discuss their implications.

2.1. Roche Radius and Ring Composition

The existence and radial extent of planetary rings are determined by the tidal field of the planet. To make this discussion more concrete, we focus on the Saturnian system. Within the planet's Roche radius, a satellite cannot attain hydrostatic equilibrium, which typically leads to mass loss and the disruption of the satellite and the subsequent formation of rings (Roche 1847;
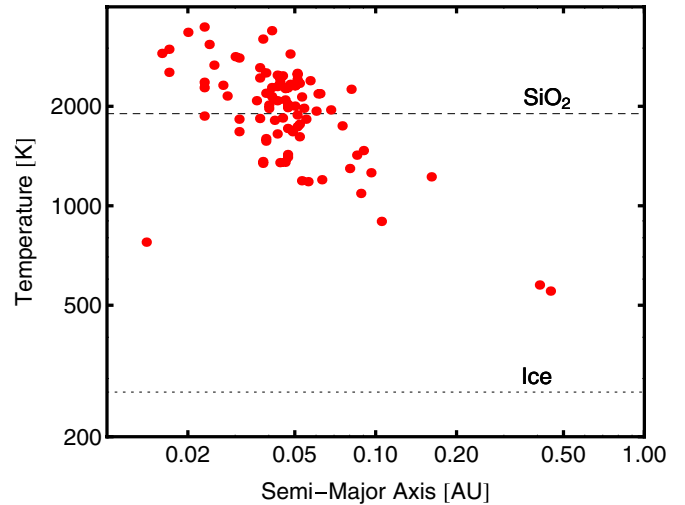
Figure 1. Equilibrium blackbody temperature for ring particles for known transiting extrasolar planets. The melting temperature of water ice (dotted line) and silicon dioxide (SiO_2; dashed line) are plotted for comparison. Exoplanet data are taken from Wright et al. (2010, http://exoplanets.org).

(A color version of this figure is available in the online journal.)

Chandrasekhar 1969). In particular, for a large, self-gravitating, and synchronously rotating satellite with a density ρ, the Roche radius, R_{Roche}, is

$$\frac{R_{\text{Roche}}}{R_{\text{p}}} = 2.45 \left(\frac{\rho_{\text{p}}}{\rho} \right)^{1/3}, \qquad (2)$$

where $\rho_{\text{p}} = 3 M_{\text{p}} / 4\pi R_{\text{p}}^3$ is the average density of the planet (Murray & Dermott 2000). For icy particles that make up the Saturnian system, the average density is 0.5–$0.9\,\text{g cm}^{-3}$, while the density of Saturn is $\approx 0.7\,\text{g cm}^{-3}$. Hence, from Equation (2), we have that Saturn's ring system should extend out to approximately twice Saturn's planetary radius, which is consistent with the observed rings around Saturn.

The icy particles that make up Saturn's rings can exist at Saturn's orbital radius because the local temperature is sufficiently low. However, for the known extrasolar planets, the presence of ices is doubtful as most of them reside close to their parent star. In Figure 1, we plot the equilibrium blackbody temperature for ring particles of known transiting extrasolar planets. All of these planets have blackbody effective temperatures well in excess of the melting temperature of water ice. There is a considerable range in melting and sublimation temperatures for different compositions of rock. For comparison we plot the melting temperature of silicon dioxide (SiO_2), which is a high-melting-point solid. Comparing the equilibrium blackbody temperatures for the currently known transiting exoplanets with the melting temperature of SiO_2 suggests that up to about 35 extrasolar planets could harbor rings made of rocky material. The blackbody equilibrium temperature shown in Figure 1 was calculated from the exoplanet's semimajor axis. Ring particles around eccentric exoplanets may therefore reach maximum temperatures that exceed the temperatures plotted in Figure 1.

The density of rock varies between 2 and 5 g cm^{-3} depending on composition, i.e., iron/nickel content, and porosity. The higher density of rock compared to ice implies that the resulting ring systems would be more compact compared to icy ring systems (see Equation (2)). Still a substantial number of extrasolar planets could potentially support rings. We show this in Figure 2

---

[5] We have used the moment of inertia of a constant density sphere $I_P = (2/5) M_p R_p^2$ for our estimates (i.e., $\alpha_P = 2/5$). The actual moment of inertia of a planet should be somewhat smaller than this because it will be centrally concentrated, i.e., its density will increase toward its center.
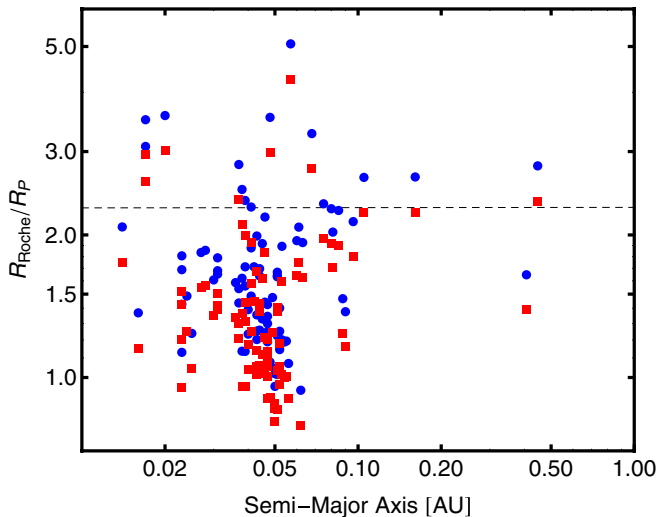
Figure 2. Roche radius, $R_{\rm Roche}$, of currently known transiting extrasolar planets for a particle density of 3 (blue circles) and 5 g cm^{-3} (red squares). The dashed line corresponds to Saturn's Roche radius with a mean density of $\rho_{\rm P} = 0.7$ g cm^{-3} and for icy ring particles with a density of $\rho = 1$ g cm^{-3}. It is clear from this plot that a significant number of extrasolar planets have Roche radii that allow for the existence of rings. The exoplanet data are taken from Wright et al. (2010, http://exoplanets.org).

(A color version of this figure is available in the online journal.)

where we plot the Roche radius of currently known transiting extrasolar planets for ring particle densities of 3 (blue circles) and 5 g cm^{-3} (red squares). We also plot $R_{\rm Roche}$ for Saturn with a mean density of $\rho_{\rm P} = 0.7$ g cm^{-3} and water ice ring particles with $\rho = 1$ g cm^{-3}. It is clear from this plot that a number of extrasolar planets can support rings made of rocky material. Indeed 86(76) of the 88 planets with reliable radius measurements can support rocky rings with a material density of $\rho = 3(5)$ g cm^{-3}, i.e., $R_{\rm Roche}/R_{\rm p} > 1$. Of these planets, 21 (12) or 24% (14%) can support sizable rings, i.e., $R_{\rm Roche}/R_{\rm p} > 2$.

2.2. Poynting–Robertson Drag

Having calculated the equilibrium temperatures and the sizes of the Roche radii of extrasolar planets, we now turn to examining the ring lifetimes due to Poynting–Robertson drag. In the solar system, Poynting–Robertson drag is not important for Saturn's rings, but it does drive the evolution of particles in Jupiter's rings (Burns et al. 1999; Showalter et al. 2008). Because of the larger stellar insolation of warm Saturns, Poynting–Robertson drag is significant even for large ring particles as we show below.

The orbital decay time, $t_{\rm PR}$, of a circumplanetary ring particle with radius, s, due to Poynting–Robertson drag is given by

$$t_{\rm PR} \sim \frac{8\rho s c^2}{3(L/4\pi a^2)Q_{\rm PR}(5+\cos^2(i))}, \qquad (3)$$

where c is the speed of light, L is the stellar luminosity, i is the inclination of the ring plane with respect to the orbital plane of the extrasolar planet, and $Q_{\rm PR}$ is the radiation pressure efficiency factor (Burns et al. 1979). If the orbital evolution of each ring particle can be considered independently and if mutual shadowing of ring particles can be neglected, then Equation (3) yields the ring particle lifetime due to Poynting–Robertson drag. Figure 3 shows the smallest ring particles that can survive over 10^8 yr in known transiting extrasolar planet systems due to Poynting–Robertson drag
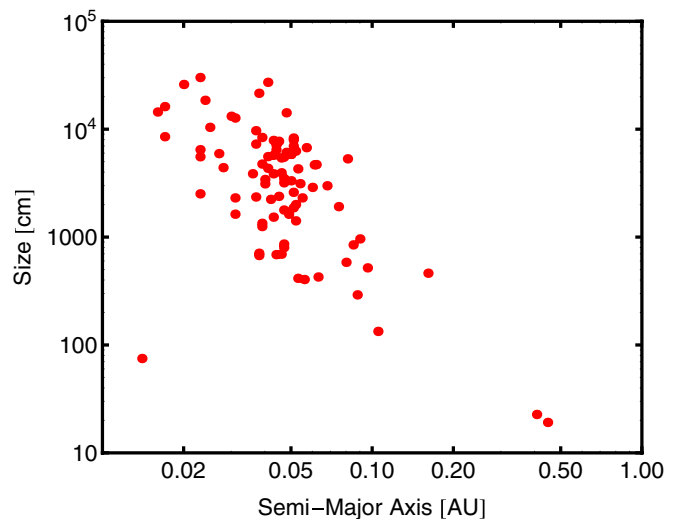

Figure 3. Smallest ring particle size for which $t_{\rm PR} > 10^8$ yr of known transiting extrasolar planets. The Poynting–Robertson timescale, $t_{\rm PR}$, was evaluated assuming $Q_{\rm PR} \sim 0.5$ and $i \sim 45°$. The exoplanet data used in this calculation are taken from Wright et al. (2010, http://exoplanets.org).

(A color version of this figure is available in the online journal.)

provided that each ring particle evolves independently. From Equation (3) we see that $t_{\rm PR}$ is considerably shorter for small ring particles, suggesting a considerable amount of ring spreading due to Poynting–Robertson drag. It is, however, likely that the evolution of individual ring particles are coupled to each other by frequent collisions, in which case the size dependence of $t_{\rm PR}$ is averaged out.

On the other hand, if the ring is optically thick, then the Poynting–Robertson drag timescale depends on the ring mass surface density instead of the sizes of individual ring particles (see Equation (4)). For an optically thick ring the maximum surface area that is exposed to stellar irradiation is $\pi \sin i (R_{\rm out}^2 - R_{\rm in}^2)$, where $R_{\rm out}$ and $R_{\rm in}$ are the outer and inner ring radii, respectively. Averaging over the orbit of the planet around the star holding the ring orientation fixed, we find that the average surface area exposed to the host star is $2 \sin i (R_{\rm out}^2 - R_{\rm in}^2)$. This yields an orbital decay time due to Poynting–Robertson drag given by

$$t_{\rm PR} \sim \frac{\pi c^2 \Sigma}{\sin i (L/4\pi a^2) Q_{\rm PR}(5+\cos^2(i))}, \qquad (4)$$

where Σ is the mass surface density of the ring. Figure 4 shows the ring lifetimes for known extrasolar planets for ring mass surface densities comparable to Saturn's B-ring (i.e., $\Sigma \sim 400$ g cm^{-2}; Robbins et al. 2010). Since $t_{\rm PR}$ scales as Σ, we note here that the ring lifetimes could be significantly longer for ring systems with ring mass surface densities larger than that of Saturn. Furthermore, the ring lifetimes in Figure 4 were calculated for an inclination of 45°, rings with smaller inclinations than this reference value would have longer lifetimes, since a smaller effective ring surface area would be exposed to the radiation from the host star.

Figure 3 suggests that ring particles, if they evolve individually, need to be about one meter and larger for the existence of long-lived rings (i.e., $t > 10^8$ yr) around the currently known transiting extrasolar planets. If, however, the ring is optically thick, then the Poynting–Robertson drag timescale depends only on the mass surface density of the ring and significantly smaller
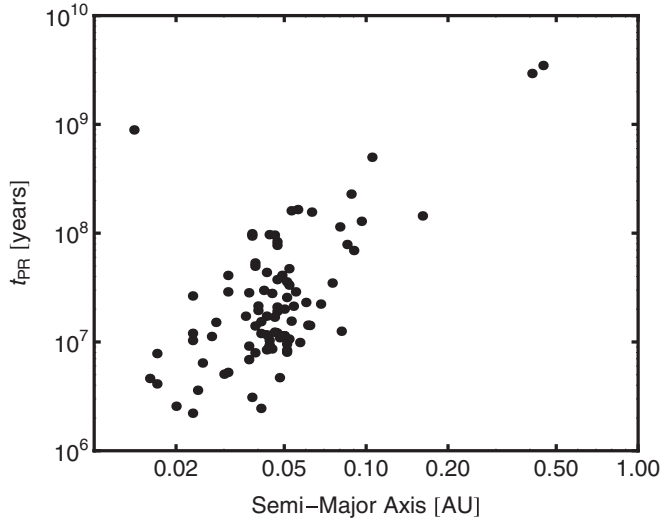
3

Figure 4. Ring lifetimes due to Poynting–Robertson drag assuming optically thick planetary rings around known transiting extrasolar planets. The Poynting–Robertson timescale, t_{PR}, was evaluated assuming $Q_{PR} \sim 0.5$, $i \sim 45°$, and $\Sigma \sim 400$ g cm^{-2}.

ring particles can survive over long periods. We note here that the actual ring lifetimes could be shortened due to ring spreading caused by collisions between ring particles, differential precession, and/or Poynting–Robertson drag (Goldreich & Tremaine 1979, 1982).

2.3. Formation

Extrasolar planets with masses comparable to Neptune and larger on short-period orbits probably did not form in situ but reached their current location by either planet–planet scattering, migration, or by Kozai oscillations with a stellar companion (e.g., Lin & Papaloizou 1979; Lin et al. 1996; Rasio & Ford 1996; Chatterjee et al. 2008; Wu & Murray 2003; Wu et al. 2007). If such planets originally had icy rings, then these rings would have been sublimated by the time they arrived at their current semimajor axes. This suggests that if extrasolar rings are discovered around such planets, they probably formed close to their current semimajor axes, which may have interesting implications for ring formation.

The Hill radius, R_H, denotes the distance from a planet at which the tidal forces from its host star and the gravitational forces from the planet, both acting on a test particle, are in equilibrium. It is given by

$$R_H = a \left(\frac{M_p}{3M_*} \right)^{1/3}. \tag{5}$$

In our solar system, planetary rings typically reside well inside the Hill sphere of their respective hosts. This is because in our solar system $R_{Roche} \ll R_H$. For some extrasolar planets however, $R_{Roche} \sim R_H$, due to the proximity to their host stars. Since the outer regions of the Hill sphere are unstable (e.g., Henon 1969, 1970; Innanen 1979; Hamilton & Burns 1991; Schlichting & Sari 2008), no planetary rings can exist there. The permitted range within which bound stable orbits, and therefore rings, can exist depends on the inclination of the ring particle's orbit. Retrograde orbits are in general more stable than prograde orbits. For example, coplanar prograde orbits are stable within about $R_H/3$, whereas coplanar retrograde orbits are stable within about $2R_H/3$ (e.g., Henon 1969; Vieira Neto & Winter 2001).

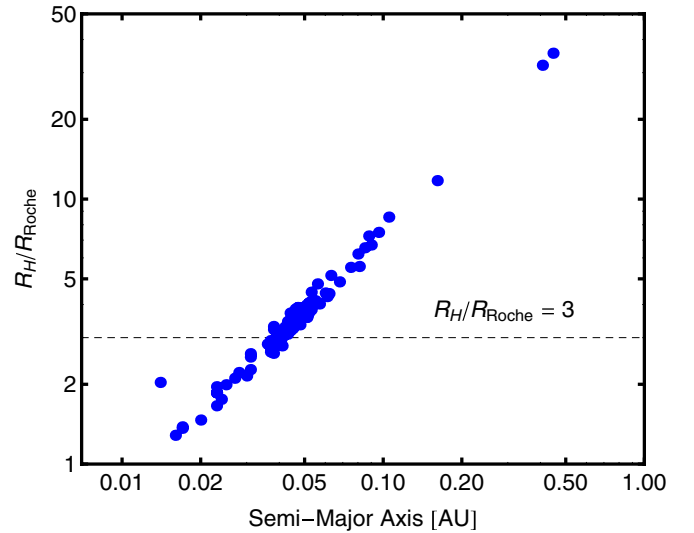**Figure 5.** Ratio of the Hill radius, R_H, to the Roche radius, R_{Roche}, of known extrasolar planets. The dashed line corresponds to $R_H/R_{Roche} = 3$. The exoplanet data are taken from Wright et al. (2010, http://exoplanets.org).

(A color version of this figure is available in the online journal.)

The unstable outer parts of the Hill sphere could have interesting implications for ring formation scenarios. If rings are formed by a larger body that sheds mass as it comes within the Roche radius of a given extrasolar planet, then extrasolar planets with $R_{Roche} \sim R_H$ are at a disadvantage, since, due to the lack of bound, stable orbits in the outer parts of the Hill sphere, mass shed in this region will be lost from the system and will therefore not be available for ring formation. Therefore, for prograde rings, an extrasolar planet with $R_{Roche} < R_H/3$ may be a better candidate for hosting rings than one with $R_{Roche} > R_H/3$ (see Figure 5).

2.4. Ring Orientation

The ring orientation for some of these warm Saturns may not be trivial, since it is determined by the competing forces of the planet's bulge and the stellar tide. Because the ratio of these forces varies as a function of the ring's distance from the planet, r, the ring's orientation follows the planet's equator at small r and follows the orbital plane at large r.

The combined effects of the planet's oblateness and the stellar tide in determining the ring orientation were first recognized by Laplace (1805). Here we use the more recent discussion of Tremaine et al. (2009, hereafter TTN). Because the strength of planetary oblateness and the stellar tide scale differently with the planet ring separation, the ring orientation varies as a function of r. The plane that this defines is known as the Laplace plane. To estimate the magnitude of this effect, we first note that the strength of the quadrupole potential arising from the planet's bulge is (TTN)

$$\Phi_p = \frac{G M_p J_2 R_p^2}{r^3} P_2(\cos\theta), \tag{6}$$

where θ is the polar angle from the rotation axis of the planet, J_2 is the quadrupole gravitational harmonic, and P_2 is a Legendre polynomial. The quadrupole potential arising from the star is

$$\Phi_* = \frac{G M_* r^2}{2a^3(1 - e_*)^{3/2}} P_2(\cos\theta_*), \tag{7}$$
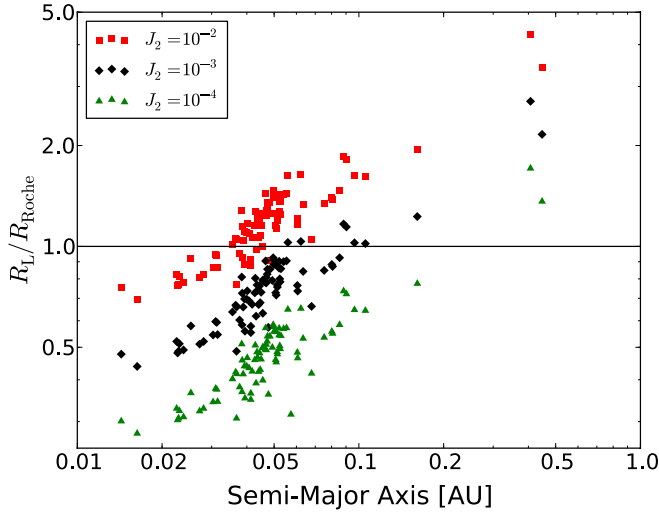
Figure 6. Ratio of the Laplace radius to the Roche radius for ring material with a density of $3\,\mathrm{g\,cm^{-3}}$ and $J_2 = 10^{-4}\text{–}10^{-2}$. The solid line marks where $R_{\mathrm{L}} = R_{\mathrm{Roche}}$. Above this line, the rings will mostly lie in the plane defined by the planet's equator, whereas below this line, the rings will undergo a transition from lying in the planet's equatorial plane at small r to lying in the orbital plane at large r. The exoplanet data used in this calculation are taken from Wright et al. (2010, http://exoplanets.org).

(A color version of this figure is available in the online journal.)

where e_* is the extrasolar planet's eccentricity. Equating Equations (6) and (7) and ignoring the P_2 terms,[6] we estimate what is known as the Laplace radius, R_{L}:

$$R_{\mathrm{L}}^5 = 2 J_2 R_{\mathrm{p}}^2 a^3 (1 - e_*)^{3/2} \frac{M_p}{M_*}. \qquad (8)$$

This simple order of magnitude estimate agrees with the exact calculation of TTN.[7] Numerically, this gives

$$\frac{R_{\mathrm{L}}}{R_{\mathrm{p}}} \approx 2.9 \left(\frac{J_2}{0.01} \right)^{1/5} \left(\frac{(a/0.1\,\mathrm{AU})}{(R_{\mathrm{p}}/R_J)} \right)^{3/5}$$
$$\times \left(\frac{M_p/M_*}{0.001} \right)^{1/5} (1 - e_*)^{3/10}, \qquad (9)$$

where $R_J = 71{,}492$ km is the radius of Jupiter. To determine if the rings will lie in the equatorial plane of the planet or in the planet's orbital plane around the host star, we take the ratio of R_{L} and R_{Roche}:

$$\frac{R_{\mathrm{L}}}{R_{\mathrm{Roche}}} \approx 0.75 \left(\frac{J_2}{0.01} \right)^{1/5} \left(\frac{M_p/M_*}{0.001} \right)^{-2/15} \left(\frac{R_{\mathrm{p}}}{R_J} \right)^{2/5}$$
$$\times \left(\frac{a}{0.1\,\mathrm{AU}} \right)^{3/5} \left(\frac{\rho}{3\,\mathrm{g\,cm^{-3}}} \right)^{1/3}. \qquad (10)$$

In Figure 6, we plot this ratio for three different values of J_2, ranging from of 10^{-4} to 10^{-2}. For reference, we note that the giant planets in the solar system have J_2's that vary from ≈ 0.003 for Uranus and Neptune to ≈ 0.01 for Jupiter and Saturn. $R_{\mathrm{L}} = R_{\mathrm{Roche}}$ is denoted by the solid line in Figure 6. Above this line, $R_{\mathrm{L}} > R_{\mathrm{Roche}}$ and the rings will mostly lie in the plane defined by the planet's equator. Below this line, $R_{\mathrm{L}} < R_{\mathrm{Roche}}$

---

[6] Another way of looking at this is to assume θ and θ_* are $\approx \pi/2$ so that $P_2(\theta, \theta_*) \approx 1/2$.
[7] TTN lack our factor of two, which is instead absorbed into their equation for the Laplace equilibria, i.e., their Equation (23).

and the rings will undergo a transition from lying in the planet's equatorial plane at small r to lying in the orbital plane at large r. From Figure 6, it is clear that the fraction of planets with nontrivial Laplacian planes varies with J_2. For $J_2 \lesssim 10^{-3}$, most ringed extrasolar planets fall below this line and thus have warped rings such that their rings will lie in the planet's equatorial plane inside of R_{L}, but coincide with the orbital plane outside of R_{L}. On the other hand, for $J_2 = 10^{-2}$, most planets have rings that lie in the plane defined by the exoplanet's equator, much like the planetary rings in the solar system.

The observational signature of warped rings is especially interesting as it provides a means by which the planet's J_2 can be measured directly. Present constraints on J_2 are inferred from transit measurements of the planet's oblateness (Carter & Winn 2010a). The inferred J_2 from such oblateness measurements is however model dependent. Since warped rings provide a direct constraint on the planet's J_2, which in turn relates to the three moments of inertia about the principle axes, the planet's internal structure can be probed (Ragozzine & Wolf 2009). Furthermore, measurements of an exoplanet's J_2 and of its oblateness would together constrain its spin period. This method was successfully applied in the past to determine the rotation period of Uranus (Dunham & Elliot 1979; Elliot et al. 1981).

3. DISCUSSION AND CONCLUSIONS

We examined the nature of rings that could exist around extrasolar planets that have orbital periods of about 1 yr or less. Such systems are ideal targets for the *Kepler* satellite, whose photometric precision will be able to identify Saturn-like rings around extrasolar planets that are transiting Sun-like stars (Barnes & Fortney 2004; http:keplergo.arc.nasa.gov/CalibrationSN.shtml).

We have shown that most currently known transiting extrasolar planets are too close to their parent star to support icy rings but that a significant fraction of them could harbor ring particles made of rock or silicates. We calculated the Roche radius for currently known transiting extrasolar planets and compared it with that of Saturn. Most currently known transiting extrasolar planets have Roche radii large enough to support rings and 12 to 21 of them have Roche radii that are comparable to or larger than Saturn's Roche radius, suggesting that such extrasolar planets could harbor sizable rings. In addition, we examined the ring lifetime due to Poynting–Robertson drag. For optically thick rings and a ring mass surface density similar to that of Saturn's B-ring, we find ring lifetimes typically range from a few times 10^6 to a few times 10^9 yr. We note here that the actual ring lifetimes could be shortened due to ring spreading (Goldreich & Tremaine 1979, 1982). Finally, we showed that, in contrast to the rings in the solar system, some of these extrasolar rings may be warped because of the competing effects of planetary and stellar tide. Observations of warped rings would provide a direct measurement of the planet's J_2. This is particularly exciting, since a planet's J_2 reveals information about its interior structure (Ragozzine & Wolf 2009). Previous constraints on the J_2 of extrasolar planets are model dependent as they are derived from the exoplanet's oblateness, which is determined from transit light curves (Seager & Hui 2002; Barnes & Fortney 2003; Carter & Winn 2010b; Leconte et al. 2011). For example, Carter & Winn (2010a) recently placed constraints on the J_2 of HD 189733b to be <0.068. Furthermore, measurements of an exoplanet's J_2 from warped rings and of its oblateness would together place limits on its spin period.

Close-in extrasolar planets with masses comparable to Neptune and larger are generally thought to have formed outside the ice line and to have reached their current location by either planet–planet scattering, disk migration, or by Kozai oscillations with a stellar companion (e.g., Lin & Papaloizou 1979; Lin et al. 1996; Rasio & Ford 1996; Chatterjee et al. 2008; Wu & Murray 2003; Wu et al. 2007). If such planets originally formed with icy rings, such rings would have been sublimated by the time they arrived at their current semimajor axes. This suggests that, if extrasolar rings are discovered, they probably formed close to their current location. We showed that due to the proximity to their host stars, $R_{\rm Roche} \sim R_{\rm H}$ for some extrasolar planets. This has interesting implications for ring formation, since orbits in the outer regions of the Hill sphere are chaotic and often unbound, which makes this region unsuitable for harboring rings. If rings are formed by a larger body that sheds mass as it comes within the Roche radius of a given extrasolar planet, then extrasolar planets with $R_{\rm Roche} \sim R_{\rm H}$ are at a disadvantage, since, due to the lack of bound, stable orbits in the outer parts of the Hill sphere, mass shed in this region will be lost from the system and will therefore not be available for ring formation. Therefore, an extrasolar planet with $R_{\rm Roche} \ll R_{\rm H}$ may be a better candidate for hosting rings than one with $R_{\rm Roche} \sim R_{\rm H}$.

The observation of extrasolar rings can offer interesting constraints on the obliquity distribution of extrasolar planets. These insights, in turn, may help to differentiate between various proposed mechanisms by which these warm Saturns were transported to their current location. For example, if planet–planet scattering (Rasio & Ford 1996; Chatterjee et al. 2008) and/or Kozai oscillations with a stellar companion (Wu & Murray 2003; Wu et al. 2007) are responsible for the observed small semimajor axes of many exoplanets, then the extrasolar planet's obliquities should be large. If on the other hand, migration in a gaseous disk is primarily responsible for the current location of close-in extrasolar planets then their obliquities are likely to be small (Lin & Papaloizou 1979; Lin et al. 1996). The obliquity distribution of extrasolar planets therefore provides a valuable probe for differentiating between these proposed planet formation scenarios. Recent measurements of the Rossiter–McLaughlin effect find a strong misalignment between the normal of the orbital plane and the stellar spin axis for some exoplanets (e.g., Winn et al. 2010), which is consistent with expectations from planet–planet scattering and Kozai oscillations.

Furthermore, for sufficiently small semimajor axes, stellar tides will act to damp the exoplanet's obliquity (Goldreich & Peale 1970; Hut 1981) while preserving the spin axis orientation at large semimajor axes (see Equation (1)). Hence, one may expect to see a transition from smaller to larger obliquities with increasing semimajor axis. Observations of such a transition in the obliquity distribution of exoplanets could in principle be used to infer the tidal dissipation function, Q_P. However, the actual obliquity evolution may be complicated by interactions with other planets in the system, as Laskar & Robutel (1993) have shown to be important for the terrestrial planets in the solar system. In addition, stellar tides do not need to damp the planet's obliquity to zero, because for sufficiently high initial obliquities, the planets may settle into a high-obliquity Cassini state (Winn & Holman 2005; Fabrycky et al. 2007).

In summary, given the various requirements for harboring rings and the fact that rings are most easily discovered around exoplanets with significant obliquities (Barnes & Fortney 2004; Ohta et al. 2009), we conclude that the majority of the currently known transiting extrasolar planets examined here are not ideal candidates for ring detections, since most of them are too close to their parent star. We find, however, no compelling reason arguing against the detection of rings around exoplanets with semimajor axes $\gtrsim 0.1$ AU, which is very exciting since the *Kepler* satellite will probe this parameter space.

REFERENCES

Barnes, J. W., & Fortney, J. J. 2003, ApJ, 588, 545
Barnes, J. W., & Fortney, J. J. 2004, ApJ, 616, 1193
Borucki, W. J., et al. 2010, Science, 327, 977
Burns, J. A., Lamy, P. L., & Soter, S. 1979, Icarus, 40, 1
Burns, J. A., Showalter, M. R., Hamilton, D. P., Nicholson, P. D., de Pater, I., Ockert-Bell, M. E., & Thomas, P. C. 1999, Science, 284, 1146
Carter, J. A., & Winn, J. N. 2010a, ApJ, 709, 1219
Carter, J. A., & Winn, J. N. 2010b, ApJ, 716, 850
Chandrasekhar, S. (ed.) 1969, Ellipsoidal Figures of Equilibrium (New Haven, CT: Yale Univ. Press)
Chatterjee, S., Ford, E. B., Matsumura, S., & Rasio, F. A. 2008, ApJ, 686, 580
Dunham, E., & Elliot, J. L. 1979, BAAS, 11, 568
Elliot, J. L., French, R. G., Frogel, J. A., Elias, J. H., Mink, D. J., & Liller, W. 1981, AJ, 86, 444
Fabrycky, D. C., Johnson, E. T., & Goodman, J. 2007, ApJ, 665, 754
French, R. G., & Nicholson, P. D. 2000, Icarus, 145, 502
Goldreich, P., & Peale, S. J. 1970, AJ, 75, 273
Goldreich, P., & Tremaine, S. 1979, Nature, 277, 97
Goldreich, P., & Tremaine, S. 1982, ARA&A, 20, 249
Hamilton, D. P., & Burns, J. A. 1991, Icarus, 92, 118
Henon, M. 1969, A&A, 1, 223
Henon, M. 1970, A&A, 9, 24
Hut, P. 1981, A&A, 99, 126
Innanen, K. A. 1979, AJ, 84, 960
Jackson, B., Greenberg, R., & Barnes, R. 2008, ApJ, 678, 1396
Laplace, P. S. 1805, Mécaniqe Céleste, Vol. 4, Book 8 (Paris: Courcier)
Laskar, J., & Robutel, P. 1993, Nature, 361, 608
Leconte, J., Lai, D., & Chabrier, G. 2011, A&A, 528, A41
Levrard, B., Correia, A. C. M., Chabrier, G., Baraffe, I., Selsis, F., & Laskar, J. 2007, A&A, 462, L5
Lin, D. N. C., Bodenheimer, P., & Richardson, D. C. 1996, Nature, 380, 606
Lin, D. N. C., & Papaloizou, J. 1979, MNRAS, 186, 799
Murray, C. D., & Dermott, S. F. 2000, Solar System Dynamics (Cambridge: Cambridge Univ. Press)
Ohta, Y., Taruya, A., & Suto, Y. 2009, ApJ, 690, 1
Ragozzine, D., & Wolf, A. S. 2009, ApJ, 698, 1778
Rasio, F. A., & Ford, E. B. 1996, Science, 274, 954
Robbins, S. J., Stewart, G. R., Lewis, M. C., Colwell, J. E., & Sremčević, M. 2010, Icarus, 206, 431
Roche, R. A. 1847, Mem. Sect. Sci., 1, 243
Schlichting, H. E., & Sari, R. 2008, ApJ, 686, 741
Seager, S., & Hui, L. 2002, ApJ, 574, 1004
Showalter, M. R., de Pater, I., Verbanac, G., Hamilton, D. P., & Burns, J. A. 2008, Icarus, 195, 361
Tremaine, S., Touma, J., & Namouni, F. 2009, AJ, 137, 3706
Vieira Neto, E., & Winter, O. C. 2001, AJ, 122, 440
Winn, J. N., Fabrycky, D., Albrecht, S., & Johnson, J. A. 2010, ApJ, 718, L145
Winn, J. N., & Holman, M. J. 2005, ApJ, 628, L159
Wright, J. T., et al. 2010, arXiv:1012.5676
Wu, Y., & Murray, N. 2003, ApJ, 589, 605
Wu, Y., Murray, N. W., & Ramsahai, J. M. 2007, ApJ, 670, 820